UNIVERSITI MALAYSIA PERLIS
International Journal of Nanoelectronics and Materials
IJNeaM
ISSN 1985-5761 | E-ISSN 2232-1535

Kinetics and Reduction Mechanism from The Carboiodination Reaction of Ilmenite Ore with Different Carbon Reductants

Nur Farhana M. Yunos[a,b,*], M. Asri Idris[b,c], Norzilah A. Halif[b,c], S. R. R. Munusamy[b,c], N. A. Nasrun[c], A. A. Adel[d], and T. Nomura[e]

[a]*Faculty of Mechanical Engineering & Technology, Universiti Malaysia Perlis (UniMAP), 02600 Arau, Perlis, Malaysia*
[b]*Frontier Materials Research, Centre of Excellence (FrontMate), Universiti Malaysia Perlis (UniMAP), 02600 Arau, Perlis, Malaysia*
[c]*Faculty of Chemical Engineering & Technology, Universiti Malaysia Perlis (UniMAP), 02600 Arau, Perlis, Malaysia*
[d]*Department of Industrial and Manufacturing Systems Engineering, Taiz University, Taiz, Yemen*
[e]*Centre for Advanced Research of Energy and Materials, Hokkaido University, Kita 13 Nishi 8 Kita-Ku Sapporo 060-8628, Japan*
∗ Corresponding author. Tel.: +601-92302319; e-mail: farhanadiyana@unimap.edu.my

Received 9 September 2025, Revised 9 October 2025, Accepted 27 October 2025

ABSTRACT

The extraction of titanium (Ti) from ilmenite ($FeTiO_3$) using carboiodination offers a potential method for selective and environmental green processing, especially when employing renewable carbon sources. This study examines the reduction behaviour and kinetics of ilmenite using carboiodination, with graphite and palm-based char serving as the carbonaceous reductants. The experimental procedure was conducted in a vertical tube furnace maintained at 1000 °C under an inert argon atmosphere to ensure controlled reaction conditions. The reaction kinetic analysis was calculated based on first-order kinetic reduction from the gas produced [carbon monoxide (CO) and carbon dioxide (CO_2)] during the reduction process by the gas analyser, while Scanning Electron Microscopy/ Energy-Dispersive X-ray Spectroscopy (SEM/ EDS) analysed the reduction mechanism. Palm char (PC-I) obtained the greatest reaction rate constant (0.002298 moles/s) and yielded 35.7 mass% Ti at 1000 °C, contrary to graphite (G-I), which produced 27.6 mass% Ti. The carboiodination reaction involves the formation of volatile titanium tetraiodide (TiI_4) via the reaction of titanium dioxide (TiO_2) with carbon (C) and iodine (I_2). PC-I's enhanced performance compared to G-I is attributed to its high surface area, porosity, and catalytic mineral content, which facilitate redox reactions and lower activation energy. The findings indicate palm char's promise as a sustainable alternative to fossil-based reductants in ilmenite reduction.

Keywords: *Carboiodination, Kinetics and reduction mechanism, Ilmenite, Graphite, Palm char*

1. INTRODUCTION

The extraction of titanium from ilmenite is a process of critical industrial importance due to the widespread applications of titanium dioxide and titanium metal in aerospace, biomedical, pigment, and chemical industries. Various methods have been explored for the purification of ilmenite, including smelting, direct acid leaching, selective chlorination, and carbothermal reduction [1]–[5]. The thermo-chemical processes have seen several advancements, but still have a limited chance of yielding appreciable cost savings over existing technologies [6]. Electrochemical approaches for in-situ electrolysis and the direct reduction of TiO_2 have shown promising progress. Nevertheless, several technical challenges, such as redox cycling, material feeding, reaction kinetics, and thermal management, must be addressed before these methods can be effectively scaled for industrial use. The process and kinetics of the reduction of various ilmenites have been the subject of several investigations over the last few decades [7]–[9]. Therefore, the carboiodination reduction of ilmenite has a crucial influence on the commercial production of synthetic rutile or titanium iodide [3].

The carboiodination of ilmenite ore involves a combination of carbothermal reduction and iodination reactions to extract titanium dioxide and other valuable phases. This reduction method offers a novel pathway for upgrading ilmenite ores, leveraging the synergistic effects of carbon reduction and halogenation to enhance reaction efficiency. Moreover, this process enables the formation of volatile metal iodides such as titanium tetraiodide (TiI_4) and iron iodide (FeI_2), facilitating effective extraction and purification of titanium. The combined carbothermal and iodination reduction of ilmenite was investigated by Schlender and Adam [4]. It is demonstrated that at 950 °C, a combination of charcoal and reactive-ground natural ilmenite produces titanium (III) oxide (Ti_2O_3). At 1000 °C, a combination of thermolytic carbon and nanoanatase produced Ti_2O_3. In addition, at a reaction temperature of 900 °C, a significant quantity of TiI_4 was produced even though titanium carbide (TiC) is considered to be extremely unreactive.

The reduction mechanism of carboiodination involves a series of redox reactions between ilmenite, iodine, and carbonaceous reductants. These reactions proceed through both solid-solid and solid-gas interactions, depending on the physical state of iodine and the operating conditions. The initial reaction involves the partial reduction of ilmenite in the presence of carbon and iodine to form TiO_2, FeI_2, and CO, as shown in Equations (1) and (2), with free Gibbs (ΔG°) calculated.

$$FeTiO_3 + C + I_2(s) = FeI_2 + TiO_2 + CO(g) \quad (1)$$
$$\Delta G^\circ = 20.927 - 0.046T$$

$$FeTiO_3 + C + I_2(g) = FeI_2 + TiO_2 + CO(g) \quad (2)$$
$$\Delta G^\circ = 11.053 - 0.024T$$

As the temperature increases, more extensive reduction and halogenation occur. For instance, the formation of TiI_4, a volatile compound crucial for titanium separation, is produced in reactions involving both ilmenite and preformed TiO_2 phases, as shown in Equations (3-8). The reduction pathways indicate multiple mechanisms depending on stoichiometry and iodine phase. Equation (3) shows simultaneous reduction of ilmenite to TiI_4 and FeI_2 with CO_2 as a byproduct, whereas Equation (4) illustrates a complete metallothermic reduction yielding metallic Fe and TiI_4. Similarly, Equations (5) and (8) demonstrate the progressive iodination of TiO_2 to volatile TiI_4, accompanied by the release of either CO or CO_2. The Gibbs free energy values for these reactions decrease with temperature increase, indicating greater thermodynamic feasibility at elevated temperatures. These mechanisms highlight the importance of controlling the iodine phase and reaction conditions to optimize the formation of volatile iodides and improve titanium recovery from ilmenite via carboiodination.

$$2FeTiO_3 + 3C + 6I_2(s) = 2FeI_2 + 2TiI_4 + 3CO_2(g) \quad (3)$$
$$\Delta G^\circ = 43.158 - 0.065T$$

$$FeTiO_3 + 3C + 2I_2(s) = Fe + TiI_4(g) + 3CO(g) \quad (4)$$
$$\Delta G^\circ = 149.826 - 0.157T$$

$$TiO_2 + 2C + 2I_2(s) = TiI_4(g) + CO(g) \quad (5)$$
$$\Delta G^\circ = 82.696 - 0.83T$$

$$TiO_2 + C + 2I_2(s) = TiI_4(g) + CO_2(g) \quad (6)$$
$$\Delta G^\circ = 42.093 - 0.042T$$

$$2FeTiO_3 + 3C + 6I_2(g) = 2FeI_2 + 2TiI_4(g) + 3CO_2(g) \quad (7)$$
$$\Delta G^\circ = 51.505 - 0.053T$$

$$TiO_2 + 2C + 2I_2(g) = TiI_4(g) + 2CO(g) \quad (8)$$
$$\Delta G^\circ = 73.3258 - 0.055T$$

Carbon-based reductants play a critical role in influencing both the reduction kinetics and the development of the resulting phases during the ilmenite reduction process [10]–[12]. Each type of carbon material exhibits unique characteristics such as reactivity, porosity, and catalytic behaviour, which critically influence the reaction rate, the stability of intermediate phases, and the overall phase transformation mechanisms. Recent studies have concentrated on examining the phase transformation behaviour of ilmenite ore under both carbothermal and carboiodination reduction processes, to improve the efficiency of titanium extraction. For instance, another researcher [3] conducted an integrated thermodynamic and experimental investigation on the reduction of Perak ilmenite using graphite as a carbon source under an inert argon atmosphere. Similarly, Nasrun et al. [13] examined the potential of palm char as a renewable alternative to conventional carbon sources, performing a comparative analysis with graphite to assess its performance in the carbothermal iodination process.

This study aims to evaluate and analyse the reaction kinetics and reduction mechanism of ilmenite during carboiodination at 1000 °C using graphite and palm char as carbon sources. It investigates how the carbon source affects reaction rates by experimental measurements and phase analysis. Kinetic behaviour was examined using gas evolution data, specifically, the concentrations of CO and CO_2 generated during reduction, modelled as a first-order reaction. Real-time monitoring of gaseous species enabled the determination of rate constants, providing a quantitative basis for comparing reductant efficiency. This study aims to contribute to the development of economically viable and environmentally responsible approaches for titanium extraction from ilmenite by identifying the optimal reaction kinetics associated with various reductants.

2. METHODOLOGY

2.1. Materials Preparation

The ilmenite ore utilized in this study was obtained from the Kinta Valley region in Perak, Malaysia. The ore sample was ground using a planetary ball mill and sieved to obtain particles smaller than 63 μm. Its chemical composition was subsequently analysed using X-ray fluorescence (XRF) spectroscopy. Two carbonaceous reductants were selected for the study: commercial graphite (G-I) and palm char (PC-I), the latter derived from palm kernel shells. Palm char was produced via pyrolysis at 450 °C under a continuous nitrogen flow of 1 L/min for 2 hours, followed by grinding and sieving to achieve a particle size below 63 μm [13]. Both carbon-based reductants were characterized to evaluate their effectiveness in the carboiodination process. To further investigate the reaction mechanisms, the surface morphology and elemental composition were analysed using scanning electron microscopy coupled with energy-dispersive X-ray spectroscopy (SEM/ EDS).

Elemental CHONS analysis was performed to quantify carbon, hydrogen, oxygen, nitrogen, and sulphur content. Proximate analysis, following ASTM D4442-92 [14], ASTM E1755-01 [15], and ASTM D3172-13 [16], was used to assess fixed carbon, volatile matter, ash, and moisture. Detailed results on the composition and properties of these carbon materials are available in prior work [13].

2.2. Experimental Procedure

The carboiodination reduction experiments were conducted in a vertical quartz tube reactor as illustrated in Figure 1. The quartz wool is inserted to hold the specimen within the hot zone of the furnace and promote uniform gas distribution. Iodine solution was placed in a sealed glass container connected to the argon gas line. The container was heated using a magnetic stirrer hot plate at a temperature of 184 °C to facilitate the sublimation of iodine. The generated vapor iodine was carried into the vertical furnace by a stream of high-purity argon gas, introduced at a constant flow rate of 0.2 L/min. The ilmenite specimen was placed on quartz wool, previously mixed with a specific carbonaceous reductant, G-I and PC-I. The reactor heating was increased from room temperature to 1000 °C at a uniform heating rate of 20 °C/min. Throughout the process, the produced gases from the reaction, primarily CO and CO_2, were measured by a gas analyser, which was interfaced with a computer for real-time monitoring and data acquisition.

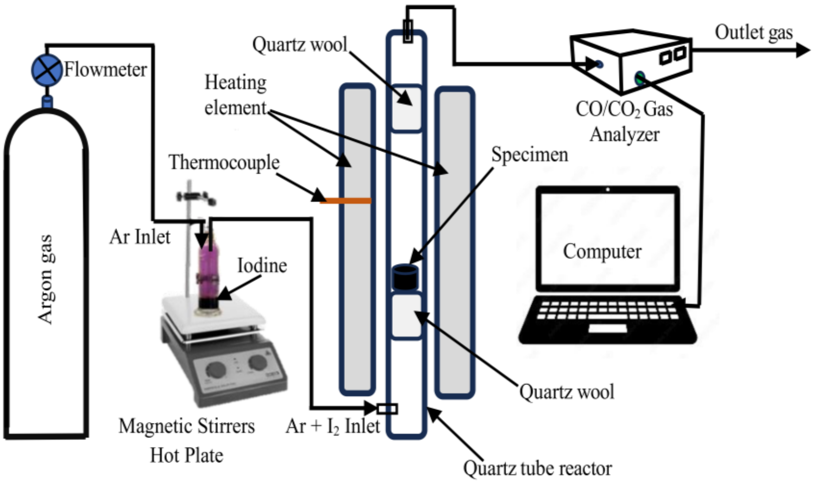

Figure 1. A schematic diagram of the carboiodination reactor at 1000 °C using argon and iodine gases.

2.3. Reaction Kinetic Analysis

The reaction kinetics were analysed based on the evolution rate of CO and CO_2 gases. A first-order reaction model was assumed. The reaction rate constant was determined using the integrated form of the first-order rate law as represented in Equation (9).

$$kt = ln\left(\frac{(CO + CO_2)_0}{(CO + CO_2)_t}\right) \tag{9}$$

where $(CO + CO_2)_0$ is the initial concentration of the gas, $(CO + CO_2)_t$ is the concentration at time t, and k is the rate constant.

The data from the gas analyser were recorded during the reaction, divided at regular intervals, and used to plot the natural logarithm of concentration versus time to extract the slope (k). The rate constants for G-I and PC-I were calculated and compared to evaluate the influence of reductant type on reaction kinetics [17].

3. RESULTS AND DISCUSSION

3.1. Kinetic Analysis

3.1.1. Activation Energy

This present study employed the isothermal method calculated from the gas measurement of CO and CO_2 produced to investigate the carboiodination reduction of ilmenite ore, as described in Equations (10) – (12) were identified using the Arrhenius equation:

$$k = A_{e}^{\frac{-Ea}{(RT)}} \tag{10}$$

$$k(T) \cdot f(a) = \frac{da}{dt} = v \tag{11}$$

$$k(T) = A \cdot \exp\left(-\frac{Ea}{R \cdot T}\right) \tag{12}$$

$$\ln k\,(T) = \ln a - \frac{Ea}{R} \cdot \frac{1}{T} \tag{13}$$

In the equations presented above, the term $k(T)$ denotes the temperature-dependent reaction rate constant, while $f(a)$ represents the differential and integral forms of the reaction mechanism, specifically modelled using the Avrami-Erofeev equation [18]. The parameters A, Ea, and R correspond to the pre-exponential factor (s^{-1}), the apparent activation energy (kJ/mole), and the universal gas constant ($kJ \cdot mole^{-1} \cdot K^{-1}$), respectively.

To determine the most suitable reaction mechanism, several kinetic models were assessed based on the strength of their linear correlation with time, t. The model demonstrating the highest degree of linearity was identified as the best representation of the gas-solid reaction pathway, as outlined in Equation (13). The plot of $\ln k\,(T)$ against $1/T$, shown in Figure 2, reveals a linear trend where the slope corresponds to $-Ea/R$, and the intercept to $\ln A$. These parameters were subsequently used to calculate the apparent activation energy and the pre-exponential factor.

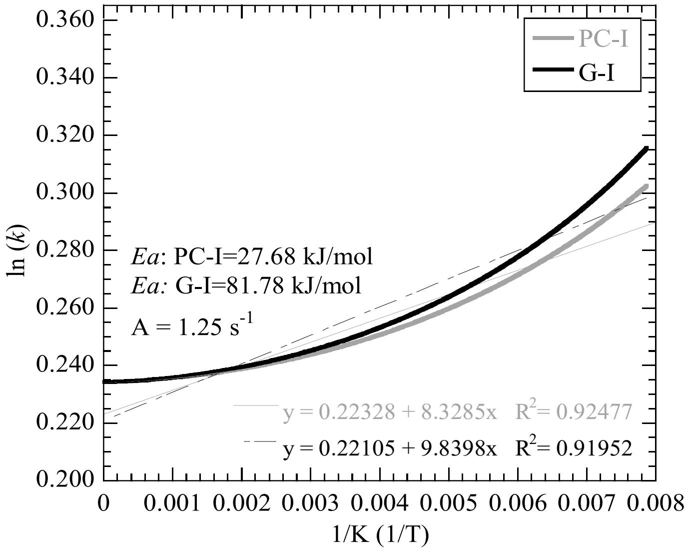

Figure 2. Variation of $ln\ (k)$ with $1/T$ for carboiodination reaction using different carbon reductants (G-I and PC-I).

Figure 2 presents the linear regression analysis of $\ln\ (k)$ versus $1/T$ across the investigated temperature range. At 1000 °C, the selected mechanism function demonstrated a strong correlation, with an R^2 value exceeding 0.91, indicating a reliable fit to the experimental data. Using Equation (13), the apparent activation energy (Ea) was determined to be 81.78 kJ/mole for the G-I sample and 27.68 kJ/mole for the PC-I sample. The corresponding pre-exponential factor A was calculated as 1.25 s^{-1} for both samples.

From the findings, under these specific reaction conditions, PC-I is the more kinetically favorable reductant, requiring less energy to reach the transition state. The lower Ea of PC-I implies a more efficient catalytic pathway, potentially due to a more reactive surface chemistry or better interaction with the reaction intermediates. These findings highlight the importance of reaction-specific behaviour in catalyst performance, where structural advantages in one context (e.g., graphitized carbon) [2], [10]. Moreover, the presence of oxygenated surface groups in PC-I can promote the initial stages of reduction by generating reactive intermediates like CO and CO_2, which synergize with iodine vapor to enhance TiI_4 formation. Setiawan et. al. [10] observed that chars derived from agricultural residues yielded lower activation energies (~217 kJ/mole) in ilmenite reduction compared to graphite (~239 kJ/mole). These results suggest that PC-I is not only more reactive under thermo-chemical conditions but also contributes to more efficient kinetics in TiO_2 extraction.

3.1.2. Reaction Rates from Carboiodination of Ilmenite Ore with Different Carbon Reductants

The carboiodination process of ilmenite using graphite and palm char as carbon reductants demonstrates distinct reduction kinetics as in Figures 3 (a) and (b). Both reductants promoted TiO_2 removal through progressive thermal treatment, as evidenced by the strong linear correlations in TiO_2 content decline ($R^2 > 0.98$), with PC-I exhibiting a steeper slope (−0.0865) than graphite (−0.0795), indicating a faster reaction rate (Figure 3 (a)). The reduction kinetics were calculated based on total oxygen removal from CO and CO_2 [17]. This behaviour can be attributed to the differences in the carbon structure and reactivity between the two materials. PC-I is characterized by a relatively high specific surface area, a significant proportion of amorphous carbon, and the presence of naturally occurring alkali and alkaline earth metals (AAEMs), including potassium (K), calcium (Ca), and magnesium (Mg) [2], [19], [20]. These minerals are known to catalyse gasification and redox reactions, promoting the formation of CO and CO_2, which are essential in facilitating the reduction of TiO_2 to volatile TiI_4 species. The underlying reaction mechanism involves initial adsorption and reaction of iodine with TiO_2 at elevated temperatures (~500–700 °C), producing intermediate suboxides (Ti_2O_3, TiO) [11], [21] and ultimately forming $TiI_{4(g)}$ via reactions such as in Equations (3 – 8).

In this context, the carbon source plays a dual role: as a reductant for $Ti^{4+} \rightarrow Ti^0$ and as a promoter for CO generation, which facilitates oxygen removal from TiO_2. Graphite, with its crystalline structure and low porosity, exhibits lower surface reactivity and fewer active sites for the reaction to initiate, thereby slowing the reduction kinetics [2]. In contrast, PC-I contains reactive surface functional groups (e.g., hydroxyl, carbonyl) and disordered carbon matrices that enhance the reactivity with oxygen species and iodine vapours [22]. Furthermore, the presence of CO and I_2 vapours contributes to a favorable gas–solid reaction mechanism, where TiI_4 formation and volatilization shift the reaction equilibrium forward, continuously driving Ti removal. The volatile TiI_4 can be condensed and collected downstream, making the process suitable for selective titanium separation [4]. Tangstad et al. [23] support this mechanistic pathway, noting that biomass-derived carbons not only improve the thermodynamics but also reduce the activation energy required for TiO_2 conversion, as in the Figure 2 result.

Overall, PC-I's catalytic constituents, high reactivity, and eco-friendly profile make it a superior alternative to graphite in the carboiodination of ilmenite, aligning with green chemistry and waste valorisation principles [10].

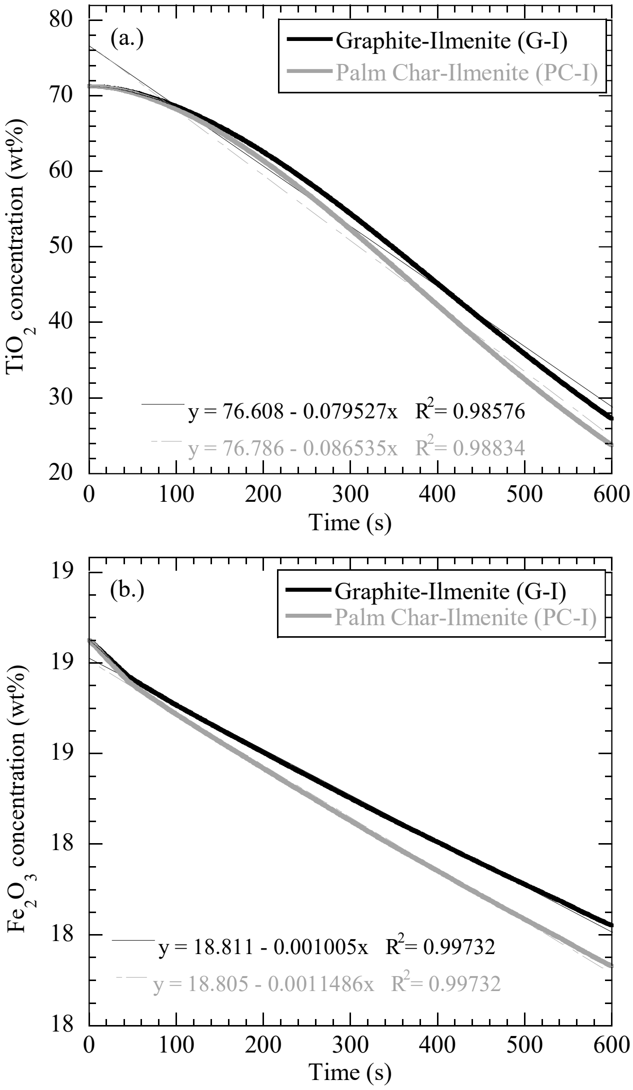

Figure 3. (a) TiO_2 and (b) Fe_2O_3 concentrations in the ilmenite ore during the carboiodination at 1000 °C for samples G-I and PC-I in 600 s of reaction.

The graph in Figure 3 (b) presents the reduction behaviour of Fe_2O_3 from ilmenite over time for two carbon reductant systems: G-I and PC-I. Both systems start with nearly identical initial Fe_2O_3 concentrations (~18.81 wt.%), but the rate of reduction differs slightly. The slope of the linear regression for PC-I (0.0011486) is steeper than that of G-I (0.001005), indicating that PC-I reduces Fe_2O_3 at a slightly faster rate under the same conditions. This result aligns with the earlier kinetic data (Figure 2), where PC-I exhibited a lower activation energy compared to G-I, suggesting a more energetically favorable reduction pathway. Ravindiran et al. [24] emphasized that the reactivity of biochar is significantly influenced by its production conditions, which affect its surface area, porosity, and functional group content, enhancing its performance in catalytic and reduction processes. The high surface activity of biochar makes it more suitable for reactions involving gas-solid interactions compared to graphitic carbons [25].

In Figure 4, the rate of reaction (*k*) of TiO_2 and Fe_2O_3 was calculated from Figure 3, demonstrating that PC-I is higher compared to G-I. The corresponding rates for the G-I were 0.002015 moles/s for TiO_2, while PC-I was 0.002298 moles/s. For Fe_2O_3, PC-I achieves a rate constant of 0.000373 moles/s, which is also notably higher than G-I's 0.000426 moles/s. These results reinforce the earlier kinetic and concentration-time analyses, confirming that PC-I is a more reactive carbon reductant under the given conditions. The reduction of metal oxides such as TiO_2 and Fe_2O_3, due to their more chemically active and structurally disordered surfaces [18].

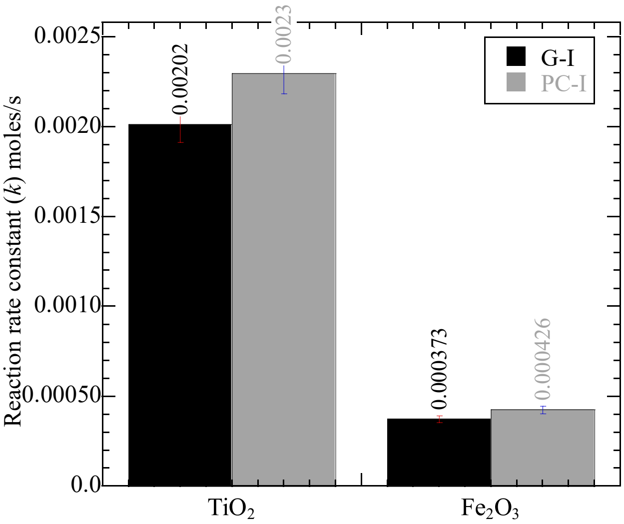

Figure 4. The reaction rate constant, *k*, of TiO_2 and Fe_2O_3 from different types of carbon reductant (G-I and PC-I) at 1000 °C through a carboiodination.

3.2. Reduction Mechanism

The SEM and EDS analysis presented in Figure 5 provides microstructural and compositional insights into the behaviour of G-I and PC-I, respectively, during the carboiodination of ilmenite ore at 1000 °C. The SEM images reveal distinct morphological differences: G-I [Figure 5 (a)] appears more compact and less porous, while PC-I [Figure 5 (b)] shows a more irregular and porous structure, which is typical of biochar-derived materials. This porous morphology in PC-I likely enhances gas-solid interactions, facilitating more efficient diffusion of reactants and products during the reduction process [10]. The EDS data further support these observations [Figure 5 (c)]. PC-I exhibits a significantly higher oxygen content (43%) compared to G-I (27.4%), suggesting either incomplete reduction or a higher retention of oxygen-containing surface groups, which are characteristic of biochar. Interestingly, PC-I also shows a higher titanium content (35.7%) than G-I (27.5%), indicating a more extensive reduction of TiO_2 in the PC-I system. This aligns with the previously discussed kinetic data (Figures 3 - 5), where PC-I demonstrated a higher reaction rate constant for TiO_2 reduction. The carbon content is slightly lower in PC-I (15%) than in G-I (15.5%), possibly due to more extensive carbon consumption during the reaction. Iron content remains nearly identical in both samples, suggesting similar extents of Fe_2O_3 reduction. This was supported by the analysis in Figure 4, where the reaction rate for both reductants was almost similar.

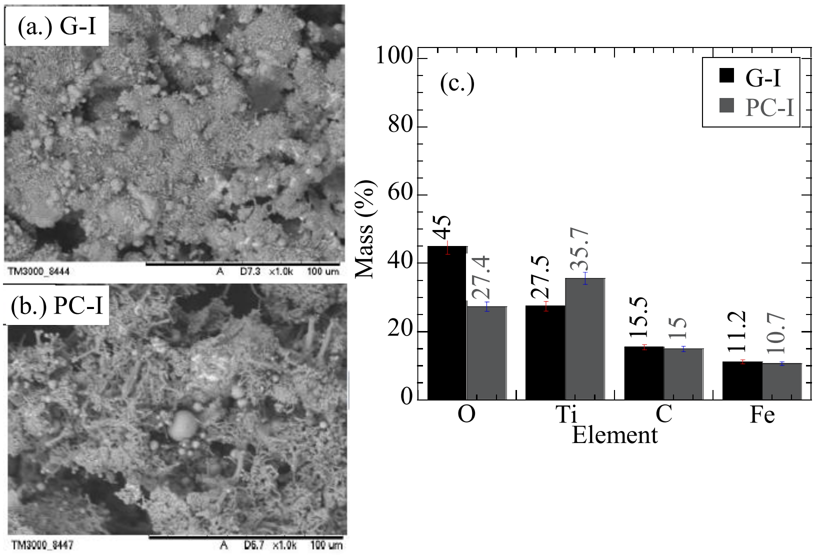

Figure 5. SEM analysis from carboiodination of ilmenite ore at 1000 °C for (a) G-I and (b) PC-I samples, and (c) EDS spectra from both samples.

The enhanced reduction performance of PC-I is attributed to its porous structure and reactive surface, consistent with studies highlighting biochar's high surface area and catalytic properties in thermal reduction processes [6], [13], [21]. The carboiodination process involves the reduction of TiO_2 in ilmenite by carbon and iodine sources to form volatile TiI_4, which can be separated from the residue. The higher TiO_2 depletion in the PC-I system suggests that the biomass-based reductant provides not only thermal and chemical reactivity but also potential cost and environmental advantages. The reaction likely proceeds via Equations (3 - 8).

4. CONCLUSION

This study demonstrates that PC-I is a more effective carbon reductant than G-I in the carboiodination of ilmenite at 1000 °C. PC-I showed a lower activation energy (27.68 kJ/mole), higher reaction rates, and greater TiO_2 reduction efficiency. Its superior performance is attributed to its porous structure, reactive surface chemistry, and catalytic mineral content. These findings support palm char as a sustainable and efficient alternative for titanium extraction.

ACKNOWLEDGMENTS

The authors acknowledge the Ministry of Higher Education Malaysia for funding this work through the Fundamental Research Grant Scheme: Phase 2020-1 (FRGS/1/2020/TK0/UNIMAP/02/30). Appreciation is also extended to the Research Management and Innovation Center (RMIC), the Faculty of Mechanical Engineering Technology, and the Faculty of Chemical Engineering Technology at Universiti Malaysia Perlis (UniMAP) for providing research facilities.

REFERENCES

[1] E. Ahmadi, S. A. Rezan, N. Baharun, S. Ramakrishnan, A. Fauzi, and G. Zhang, “Chlorination Kinetics of Titanium Nitride for Production of Titanium Tetrachloride from Nitrided Ilmenite,” *Metall. Mater. Trans. B Process Metall. Mater. Process. Sci.*, vol. 48, no. 5, 2017.

[2] Yunos N. F. M, Idris M. A, Nasrun N. A, Kurniawan A, Takahiro N, and Rezan S. A, “Structural Characterizations and Phase Transition on the Reducibility of Ilmenite Ore with Different Carbon Reductants by Carbothermal Reduction Under Hydrogen Atmosphere,” *J. Sustain. Metall.*, 2023.

[3] A. A. Adel, N. F. M. Yunos, M. A. Idris, and L. I. G. Togang, “Investigation on Phase Evaluation of Ilmenite Ore by Carbothermal Reduction and Carboiodination Reaction,” *Int. J. Nanoelectron. Mater.*, vol. 16, no. Special Issue, 2023.

[4] P. Schlender and A. E. W. Adam, “Combined Carboreduction-Iodination Reaction of TiO_2 and $FeTiO_3$ as the Basic Step toward a Shortened Titanium Production Process,” *Ind. Eng. Chem. Res.*, vol. 56, no. 23, 2017.

[5] F. Yang and V. Hlavacek, “Effective Extraction of Titanium from Rutile by a Low-temperature Chloride Process,” *AIChE J.*, vol. 46, no. 2, 2000.

[6] A. I. Mohammed, N. F. M. Yunos, M. A. Idris, Z. A. Z. Jamal, N. F. Hayazi, and T. Nomura, “Mineralogical Characterizations of Langkawi Ilmenite Ore for Carbothermal Reduction,” *Int. J. Nanoelectron. Mater.*, vol. 15, no. 1, p. 1–8, 2022.

[7] M. Chen, X. Xiao, and X. F. Zhang, “Kinetics of Carbothermic Reduction of Ilmenite,” in *Materials Science Forum*, 2016, vol. 852.

[8] N. F. M. Yunos, J. H. Chong, A. I. Mohammed, and M. A. Idris, "Phase Evolution during Carbothermal Reduction of Langkawi Ilmenite Ore at Different Reaction Times," Materials Science Forum, vol. 1010, p. 391-396, 2020.

[9] W. Lv, X. Lv, X. Lv, J. Xiang, C. Bai, and B. Song, “Non-Isothermal Kinetic Studies on the Carbothermic Reduction of Panzhihua ilmenite concentrate,” *Miner. Process. Extr. Metall. Trans. Inst. Min. Metall.*, vol. 128, no. 4, 2019.

[10] A. Setiawan, M. A. Rhamdhani, M. I. Pownceby, N. A. S. Webster, and S. Harjanto, “Kinetics and Mechanisms of Carbothermic Reduction of Weathered Ilmenite Using Palm Kernel Shell Biomass,” *J. Sustain. Metall.*, vol. 7, no. 4, 2021.

[11] M. Tripathy, S. Ranganathan, and S. P. Mehrotra, “Investigations on Reduction of Ilmenite Ore with Different Sources of Carbon,” *Trans. Institutions Min. Metall. Sect. C Miner. Process. Extr. Metall.*, vol. 121, no. 3, 2012.

[12] H. C. S. Subasinghe and A. S. Ratnayake, “Effect of Different Carbon Sources on the Conversion of Ilmenite into Synthetic Rutile via Ball Milling-Induced Carbothermic Reduction,” *J. Alloys Compd.*, vol. 954, 2023.

[13] N. A. Nasrun, N. F. M. Yunos, M. A. Idris, S. R. R. Munusamy, N. Takahiro, and S. A. Rezan, “Phase Reduction and Thermodynamic Analysis of Ilmenite Ore by Carbothermal-Iodination using Different Carbon Reductants,” *Int. J. Nanoelectron. Mater.*, vol. 16, no. Special Issue, 2023.

[14] A. D4442-92, *Test Methods for Direct Moisture Content Measurement of Wood and Wood-Base Materials*. West Conshohocken, PA: ASTM International, 2003.

[15] A. E1755-01, *Standard Test Method for Ash in Biomass*, no. Reapproved. West Conshohocken, PA: ASTM International, 2020.

[16] A. D3172-13, *Standard Practice for Proximate Analysis of Coal and Coke*, vol. 13. West Conshohocken, PA: ASTM International, 2021.

[17] M. Zaharia, N. F. M. Yunos, and V. Sahajwalla, "Recycled and Renewable Materials as Resources for Electric Arc Furnace Steelmaking," From Materials to Structures: Advancement through Innovation, p. 21-27, 2013.

[18] L. Zhao, P. Gao, B. Zhao, X. Kong, Y. Han, and Y. Li, “Low-Temperature Hydrogen Reduction of Carajás Hematite: Synergistic Effects of Kinetics and Pore Evolution,” *Int. J. Hydrogen Energy*, vol. 125, p. 56–66, 2025.

[19] A. I. Mohammed, N. F. M. Yunos, M. A. Idris, N. H. Najmi, Z. A. Z. Jamal, and T. Nomura, “Phase Transformations of Langkawi ilmenite ore during Carbothermal Reduction using Palm Char as renewable reductant,” *Chem. Eng. Res. Des.*, vol. 178, 2022.

[20] N. F. M. Yunos, A. N. Ismail, S. R. R. Munusamy, M. A. Idris, and V. Sahajwalla, “Reaction Kinetics of Palm Char and Coke with Iron Oxides in EAF Steelmaking Slag,” *J. Sustain. Metall.*, vol. 7, no. 2, p. 412–426, 2021.

[21] N. A. Nasrun, N. F. M. Yunos, M. A. Idris, N. A. Halif, and T. Nomura, “The Effect of Palm Char Properties on Malaysian Ilmenite Ores by Carbothermal Reduction,” *Arch. Metall. Mater.*, vol. 69, no. No 4, p. 1491–1499, 2024.

[22] B. Sajjadi, W. Y. Chen, and N. O. Egiebor, “A Comprehensive Review on Physical Activation of Biochar for Energy and Environmental Applications,” *Rev. Chem. Eng.*, vol. 35, no. 6, 2019.

[23] G. R. Surup, A. Trubetskaya, and M. Tangstad, “Charcoal as an Alternative Reductant in Ferroalloy Production: A review,” *Processes*, vol. 8, no. 11, p. 1–41, 2020.

[24] G. Ravindiran *et al.*, “Production and Modifications of Biochar to Engineered Materials and its Application for Environmental Sustainability: A Review,” *Biochar*, vol. 6, no. 1, p. 62, 2024.

[25] Y. Lu, Q. Wang, F. Yu, S. Zhang, and X. Zhu, “Carbothermal Reduction Synthesis of Sulfide-Modified Biochar for Heavy Metal Removal,” *Carbon Res.*, vol. 2, no. 1, p. 5, 2023.